Treatment of Human Immunodeficiency Virus Infection With Tenofovir Disoproxil Fumarate–Containing Antiretrovirals Maintains Low Bone Formation Rate, But Increases Osteoid Volume on Bone Histomorphometry

Janaina Ramalho[1], Carolina Steller Wagner Martins[1], Juliana Galvão[2], Luzia N Furukawa[1], Wagner V Domingues[1], Ivone B Oliveira[1], Luciene M dos Reis[1], Rosa MR Pereira[3], Thomas L Nickolas[4], Michael T Yin[4], Margareth Eira[5,6], Vanda Jorgetti[1,7], Rosa Moyses[1,2]

[1]Department of Nephrology, Laboratório de Investigação Médica 16, Hospital das Clinicas da Faculdade de Medicina da Universidade de Sao Paulo, SP, Brazil

[2]Post-Graduation in Medicine Department, Universidade Nove de Julho, Sao Paulo, SP, Brazil

[3]Bone Laboratory Metabolism, Rheumatology Division, Faculdade de Medicina da Universidade de Sao Paulo, Sao Paulo, SP, Brazil

[4]Department of Medicine, Columbia University Irving Medical Center, New York, NY, USA

[5]Ambulatory Division, Instituto de Infectologia Emílio Ribas, Sao Paulo, SP, Brazil

[6]Medicine Department, Universidade Cidade de São Paulo-UNICID, Sao Paulo, SP, Brazil

[7]Dialysis Division, Hospital Samaritano Americas Serviços Médicos, Sao Paulo, SP, Brazil

Abstract

Bone mineral density (BMD) loss is a known complication of human immunodeficiency virus (HIV) infection and its treatment, particularly with tenofovir disoproxil fumarate (TDF)-containing antiretroviral regimens. Although renal proximal tubular dysfunction and phosphaturia is common with TDF, it is unknown whether BMD loss results from inadequate mineralization. We evaluated change in BMD by dual-energy X-ray absorptiometry (DXA) and bone histomorphometry by tetracycline double-labeled transiliac crest biopsies in young men living with HIV before ($n = 20$) and 12 months after ($n = 16$) initiating TDF/lamivudine/efavirenz. We examined relationships between calciotropic hormones, urinary phosphate excretion, pro-inflammatory and pro-resorptive cytokines, and bone remodeling-related proteins with changes in BMD and histomorphometry. Mean age was 29.6 ± 5.5 years, with mean CD4 + T cell count of 473 ± 196 cells/mm^3. At baseline, decreased bone formation rate and increased mineralization lag time were identified in 16 (80%) and 12 (60%) patients, respectively. After 12 months, we

detected a 2% to 3% decrease in lumbar spine and hip BMD by DXA. By histomorphometry, we observed no change in bone volume/total volume (BV/TV) and trabecular parameters, but rather, increases in cortical thickness, osteoid volume, and osteoblast and osteoclast surfaces. We did not observe significant worsening of renal phosphate excretion or mineralization parameters. Increases in PTH correlated with decreased BMD but not histomorphometric parameters. Overall, these data suggest abnormalities in bone formation and mineralization occur with HIV infection and are evident at early stages. With TDF-containing antiretroviral therapy (ART), there is an increase in bone remodeling, reflected by increased osteoblast and osteoclast surfaces, but a persistence in mineralization defect, resulting in increased osteoid volume.

Keywords

Introduction

The success of antiretroviral therapy (ART) has led to prolonged life expectancy in people living with human immunodeficiency virus (HIV)/acquired immunodeficiency syndrome (AIDS) (PLWH); however, comorbidities associated with aging, including osteoporosis and fracture, appear to occur in PLWH at an earlier age than in the general population.[1–5] Initiation of ART is also associated with decreases in BMD occurring within the first 6 to 12 months, ranging between 2% and 6% with different ART regimens. Despite stabilizing or increasing after the first year, BMD typically does not return to pre-ART levels.[6–11] Low BMD observed by dual-energy X-ray absorptiometry (DXA) may result either from decreased bone volume with microarchitectural deterioration, which is characteristic of age-related osteoporosis, or from impaired bone mineralization, which is characteristic of osteomalacia.[12] Because osteomalacia is a histologic diagnosis and may occur in the absence of laboratory and radiologic abnormalities,[13] a definitive diagnosis may require a bone biopsy. Tenofovir disoproxil fumarate (TDF)-based ART has been associated with greater reductions in BMD compared to non-TDF containing regimens.[7,10,11,14] Numerous case reports and observational studies have highlighted the risk of proximal tubular renal dysfunction associated with TDF use.[15–18] Therefore, it has been hypothesized that increased phosphaturia, metabolic acidosis, and decreased renal production of $1,25(OH)_2$ vitamin D resulting from renal tubulopathy might impair bone mineralization, and may in part explain the role of TDF-related BMD loss.[19,20] However, there are no definitive studies on the effect of TDF on bone mineralization utilizing bone histomorphometry. Therefore, we investigated changes in bone histomorphometry, bone expression of genes and proteins related with inflammation, proximal tubular renal function, and phosphate homeostasis in ART-naive PLWH, before and 12 months after treatment with a fixed dose combination of TDF, lamivudine, and efavirenz (TDF/3TC/EFV). We hypothesized that TDF/3TC/EFV therapy would result in impaired bone mineralization, and that changes in mineralization parameters would be related to increased renal phosphate excretion.

Patients and Methods

Study sample and biochemical measurements

ART-naive male PLWH aged 18 to 40 years attending the Instituto de Infectologia Emilio Ribas (IIER) outpatient service, Sao Paulo, Brazil, and initiating standard first-line treatment with TDF/3TC/EFV were invited to participate. Exclusion criteria included: prior ART-exposure; recent extended bed rest; diagnosis of metabolic bone disease; estimated glomerular filtration rate less than 60 mL/min/1.73 m^2; evidence of liver failure, cirrhosis, diabetes, or other endocrine diseases; and use of medications affecting bone metabolism. From February 2015 to August 2016, 26 ART-naive men with HIV agreed to participate in the protocol and signed informed consent. Six participants were excluded before the initial workup (three withdrew consent, two failed to take tetracycline, and one was diagnosed with primary hyperparathyroidism). From 20 participants who underwent baseline evaluation, four were further excluded (one needed corticosteroids after ART initiation, one reported anabolic steroids use after ART initiation, and two were lost to follow-up). Sixteen completed evaluation at 12 months and were included in follow-up analysis.

Fasting blood samples and random spot urine were collected for all participants before ART initiation and after 6 and 12 months. Serum and plasma aliquots were prepared and stored at−180°C in liquid nitrogen. Comprehensive metabolic panels and urinary phosphate, uric acid, protein, and creatinine were measured using standard assays. Urinary β2-microglobulin was determined by chemiluminescence. Fractional excretion of phosphate (FEP), fractional excretion of uric acid (FEUA), urinary protein-to-creatinine and β2-microglobulin-to-creatinine ratios, and the presence of glycosuria were investigated as markers of proximal renal tubular function. Plasma PTH was measured by chemiluminescent immunoassay (reference value: 15–65 pg/mL; Roche Diagnostics, Indianapolis, IN, USA), as were 25(OH) vitamin D (25(OH)D; LIAISON®; DiaSorin, Stillwater, MN, USA), 1,25(OH)$_2$ vitamin D (1,25(OH)$_2$D; LIAISON®; DiaSorin, Stillwater, MN, USA), and the bone turnover markers C-terminal telopeptide of type 1 collagen (CTX; reference value for men 50 to 70 years: 0.7 ng/mL; Roche Diagnostics, Indianapolis, IN, USA) and N-terminal propeptide of type 1 collagen (P1NP; reference values for men: 13.9–85.5 ng/mL; Roche Diagnostics, Indianapolis, IN, USA). The study protocol was approved by Faculdade de Medicina da Universidade de Sao Paulo and by IIER Ethics Committees, and written informed consent was obtained from all participants.

BMD measurements

BMD (g/cm^2) was measured using DXA (Hologic Disc Hologic Inc., Bedford, MA, USA) at the lumbar spine (L$_1$–L$_4$), hip (total hip and femoral neck), and radius (1/3 distal and ultradistal), according to the manufacturer's suggested guidelines. Images were obtained at the Bone Metabolism Laboratory of the Rheumatology Division, Hospital das Clínicas da Faculdade de Medicina da Universidade de São Paulo (HCFMUSP). Measurements were performed by the same trained technician, who was certified by the International Society of Clinical Densitometry (ISCD). Precision error for BMD measurements at the lumbar spine and right hip was determined by using data from 15 subjects scanned three times, with repositioning of the subject after each scan according to standard ISCD protocols.[21] The

least significant change (LSC) with 95% confidence in our laboratory was 0.033 g/cm^2 at the anteroposterior spine, 0.047 g/cm^2 at the right femoral neck, and 0.039 g/cm^2 at the right total hip. Z-score -2 was defined as below the expected range for age according to ISCD official positions for males younger than age 50 years.[22]

Transiliac bone biopsy and histomorphometry

Each participant underwent iliac crest bone biopsy after double labeling with tetracycline (20 mg/kg/day) for 3 days, separated by an interval of 10 days, with the biopsy being performed 2 to 5 days after the last dose of tetracycline. A bone specimen was obtained using a 7-mm Bordier trephine, and a second one was obtained through a 11 G $\times$ 10 bone marrow biopsy needle. The second specimen was immediately frozen at$-80°$ for further analysis of protein quantification and gene expression. Undecalcified bone fragments were processed for histological studies. Bone histomorphometry was analyzed using a semiautomatic technique in the Osteomeasure software (Osteometrics, Atlanta, GA, USA). The static and dynamic parameters were examined according to the standards established by the American Society of Bone and Mineral Research (ASBMR).[23] Reference values used for static parameters were our normal laboratory controls, obtained from 69 healthy men aged 32.9 ± 2.4 years concomitantly with the postmortem examination performed by a pathologist.[24] Ranges for the dynamic parameters were those described in men from a healthy Danish sample.[25]

Immunohistochemistry

For immunohistochemical evaluation, bone tissue sections were deacrylated and submitted to a quick semi-decalcification.[26] Then, endogenous peroxidase inhibition was performed with 3% hydrogen peroxide solution and methanol for 30 min, followed by blocking with casein-based Protein Block solution for 15 min (Protein Block; DAKO Corporation, CA, USA). The sections were then incubated overnight with the primary antibody (goat anti-OPG and goat anti-RANK-L, 1:80 dilution; Santa Cruz Biotechnology, Inc., Santa Cruz, CA, USA) in a humidified chamber at 4°C. The next day the sections were incubated with biotinylated anti-goat at the dilution of 1: 100 (BA 1000; Vector Laboratories Inc, CA, USA) and then with ABC-HRP (Vector Laboratories Inc, CA, USA) according to manufacturer's instructions. Antigen–antibody complexes were visualized using a 3-amino-9-ethylcarbazole substrate chromogen (AEC) (Sigma Chemical, St. Louis, MO, USA). The sections were rinsed in distilled water, counterstained with Mayer's Hemalum solution (Merck, Darmstadt, Germany) and analyzed under an optical microscope. The expression of receptor activator of nuclear factor kappa-B ligand (RANKL) and osteoprotegerin (OPG) was evaluated in osteocytes of the trabecular region and in osteoblasts and lining cells in the bone marrow near the trabeculae. The results were expressed as number of RANKL + or OPG + osteocytes per mm^2 of bone area, and in the number of RANKL + or OPG + osteoblasts/ lining cells per mm^2 of total area, the total area consisting of bone trabeculae and bone marrow.

Multiplex protein quantification

Metal Bead tubes 2.8 mm (OMNI International, Kennesaw, GA, USA) were used for tissue homogenization and were shaken for 3 cycles of 60 s at Bead Ruptor (OMNI International,

Kennesaw, GA, USA). Total protein was extracted from bone samples with TRIzol reagent (Invitrogen, Carlsbad, CA, USA) according to the manufacturer's instructions. In the protein lysate, RANKL, OPG, sclerostin (Scl), fibroblast growth factor (FGF)-23, tumor necrosis factor (TNF)-α, interleukin-6 (IL-6), and interleukin-1β (IL-1β) were quantified using the MILLIPLEX MAP kits Human Bone Magnetic Bead Panel (HBNMAG- 51 K) and HUMAN RANKL Magnetic Bead (HRNKLMAG-51K-01) (EMD Millipore Corporation, Billerica, MA, USA) according to the manufacturers. The same assays were used for serum protein quantification.

Gene expression

After total RNA extraction, its amount was determined by the Nano Drop 1000 spectrophotometer (Thermo Fisher Scientific, Waltham, MA, USA). The complementary DNA was synthesized from the total RNA by reverse transcriptase (Improm-II Reverse Transcriptase; Promega Corporation, Madison, WI, USA) using thermocycler (DNA Engine; MJ Research, Waltham, MA, USA). Gene expression was determined by quantitative polymerase chain reaction from the complementary DNA using the SYBR Green method (Rotor Gene SYBR Green PCR kit; Qiagen, Hilden, Germany) and the Rotor-Gene Q thermocycler (Qiagen, Hilden, Germany). The genes analyzed were FGF-23 (ACC# NM_020638.2), SOST (ACC# AF_331844.1), RANKL (ACC# NM_003701.3), OPG (ACC# U94332), RANK (ACC# NM_003839.3), IL-6 (ACC# NM_000600), TNF-α (ACC# NM_000594), IL-1β (ACC#NM_000576), and the normalizing gene GAPDH (glyceraldehyde-3-phosphate dehydrogenase; ACC# NM_002046.4) with their respective primers, which were designed by the Integrated DNA Technologies program. Data from seven healthy males aged 44.3 ± 8.8 years who died from trauma were used as controls. The gene expression was calculated by the comparative threshold (Ct) method of relative quantification. After comparison of PCR efficiency between target and reference genes, the Ct values of the target gene for each participant sample as well as for the calibrator sample were determined. Next, the Ct value for each sample was determined by subtracting the Ct value of the calibrator from the Ct value of the sample and normalized target gene expression was calculated by using the formula: 2^{-Ct}. Values are expressed as a multiple of (fold of) the expression found in healthy control cells.

Statistical analysis

Continuous variables were summarized using medians and interquartile ranges (IQRs) or means and standard deviations (SDs) as appropriate, whereas categorical variables were summarized as frequencies and percentages. When necessary, nonparametric variables were log-transformed prior to analyses. Student's t tests for paired samples and Wilcoxon signed-rank tests were used to compare parametric and nonparametric data before and after treatment, respectively. Associations among laboratory, DXA, and histomorphometric parameters were evaluated by Spearman correlation coefficients. Values of $p < 0.05$ were considered statistically significant. Statistical analyses were performed using IBM SPSS Statistics, version 20 software (IBM Corp., Armonk, NY, USA).

Results

Demographics, HIV, and immune parameters

Among the 20 men enrolled, mean age was 29.6 ± 5.5 years, BMI was 24.7 ± 2.4 kg/m^2, mean CD4 + T cell count was 473 ± 196 cells/mm^3, and mean HIV RNA was $73,580 \pm 129,221$ copies/mL. Only one participant had a CD4 + T cell count below 200 cells/mm^3, and only one other participant had an AIDS defining condition (pulmonary tuberculosis) at baseline. Among participants, nine were current smokers, one reported use of three or more units of alcohol/day, one was co-infected with hepatitis B virus, and none were co-infected with HCV. After 12 months of ART, mean CD4 + increased to 739 ± 232 cells/mm^3 and all participants had HIV viral loads below the limit of detection (< 40 copies/ml) (Table 1). Serum levels of the inflammatory cytokines, TNF-α and IL-6, decreased from baseline to 12 months (2.29, IQR 1.78–3.37 versus 1.61, IQR 1.42–2.05 pg/mL, $p = 0.03$, and 1.32, IQR 0.76–2.56 versus 1.02, IQR 0.93–1.11 pg/mL, $p = 0.06$, respectively).

Calciotropic hormone, bone turnover markers, RANKL/OPG, and sclerostin

At baseline, mean 25(OH)D was 23.0 ± 8.0 ng/mL with eight participants having levels < 20 ng/mL. Six months after initiation of ART, there was a significant increase in PTH from baseline (31.3 ± 9.2 versus 39.4 ± 12.2 pg/mL, $p = 0.03$), which stabilized and remained higher than baseline at 12 months (Table 1). Mean 25(OH)D but not 1,25(OH)2D levels, increased over 12 months while FGF-23 levels decreased (Table 1). There were no significant changes in the levels of serum phosphate, and none developed hypophosphatemia. Similarly, there were no significant changes in FEP, FEAU, urinary protein-to-creatinine, or β2-microglobulin-to-creatinine ratios, and no participant developed FEP > 18%, hypouricemia, FEAU > 15%, or glycosuria 12 months after treatment initiation.

At 6 months, bone turnover markers were also higher than baseline: osteocalcin (23.3 ± 5.9 versus 18.4 ± 5.4 ng/mL, $p = 0.01$), CTX (0.67, IQR 0.58–0.87 versus 0.41, IQR 0.25–0.62 ng/mL, $p = 0.001$), and P1NP (69.3, IQR 54.1–94.7 versus 60.1, IQR 39.9–78.9 ng/mL, $p = 0.01$). At 12 months, osteocalcin was elevated relative to baseline whereas CTX and P1NP did not differ from baseline (Table 1). Serum RANKL levels decreased from baseline to 12 months, but OPG and sclerostin levels did not differ from baseline (Table 1).

Bone mineral density by DXA

Of the 20 participants who performed DXA at baseline, three participants had Z-score   −2 at the lumbar spine, and one had Z-score   −2 at the 1/3 distal radius; none had Z-score   −2 at other skeletal sites. Distribution of DXA results did not differ for the 16 participants who had follow-up studies. At 6 months, we observed similar percentage declines in BMD at femoral neck and lumbar spine, although only femoral neck BMD change reached statistical significance (0.887 ± 0.145 versus 0.874 ± 0.136 g/cm^2, $p = 0.007$). At 12 months, BMD decreased approximately 2.1% at the lumbar spine (0.981 ± 0.094 versus 0.960 ± 0.110 g/cm^2, $p = 0.048$), 2.8% at the femoral neck (0.887 ± 0.145 versus 0.862 ± 0.145 g/cm^2, $p = 0.001$), and 1.8% at the total hip (1.029 ± 0.138 versus 1.010 ± 0.138 g/cm^2, $p = 0.04$) compared to baseline (Fig. 1A). In contrast, BMD at the predominantly cortical 1/3 distal radius remained stable over the course of ART treatment.

Bone histomorphometry

We compared baseline histomorphometric data before ART initiation in 20 participants with data from a reference population.[24,25] We observed low trabecular volume (BV/TV) in four (20%), thinned cortices in five (25%), and reduced osteoid thickness (O.Th) in 10 participants (50%). Osteoclast surface (Oc.S/BS) and eroded surface (ES/BS) were elevated in seven (40%) and five (30%) participants, respectively. Decreased bone formation rate (BFR/BS) was observed in 16 participants (80%), whereas mineralization lag time (Mlt) was higher in 12 participants (60%). We also evaluated relationships by Spearman correlations between HIV RNA levels and histomorphometry: higher HIV RNA level was associated with higher levels bone formation measures, including O.Th (0.58, $p = 0.008$), OV/BV (rho 0.58, $p = 0.007$), OS/BS (rho 0.52, $p = 0.02$), and dynamic parameters, including mineralizing surface (MS/BS; rho 0.54, $p = 0.01$) and BFR/BS (rho 0.49, $p = 0.03$), but not with other histomorphometric parameters. There were no correlations between CD4 + T cell counts and pretreatment histomorphometric data.

We evaluated changes in histomorphometry and bone-tissue level gene expression 12-months after initiation of ART ($n = 16$, Table 2). Among structural parameters, only cortical thickness (Ct.Th) increased significantly from baseline (37% increase, Table 2). Among bone formation and resorption parameters, we observed an increase in osteoid volume (OV/BV; 185%), osteoblast surface/bone surface (Ob.S/BS; 234% increase), and Oc.S/BS (121% increase). Although the increase in OV/BV was still within the reference range, Ob.S/BS and Oc.S/BS increased to values above the normal ranges. We did not observe any significant changes in dynamic parameters (MS/BS, BFR/BS, mineral apposition rate, and Mlt) from baseline (Table 2). Overall, the percentage of participants with abnormal histomorphometric parameters was not significantly different compared with baseline; however, the responses were relatively heterogeneous between individuals (Fig. 2A–F).

Figure 2 depicts individual-level changes in histomorphometry parameters from baseline to 12 months with the reference ranges for Ob.S/BS, OV/BV, Oc.S/BS, ES/BS, BFR/BS, and Mlt. For BFR/BS, the majority of participants had BFR/BS below the reference range before and after ART; eight participants had an increase in BFR/BS, none to normal values. For ES/BS, the response was more heterogeneous with approximately 69% demonstrating an increase at 12 months. Change in Ob.S/BS and Oc.S/BS were the most consistent, with approximately 69% and 75% participants, respectively, demonstrating an increase at 12 months. All participants but two had OV/BV within the reference range at baseline and the 75% had an increase from baseline. At baseline, almost all participants had abnormal Mlt, higher than the reference, without apparent change over 12 months. One participant had a dramatic 900% rise in Mlt from baseline to 12 months that was attributed to a decline in vitamin D levels (from 26 ng/mL at baseline to 12.6 ng/mL at 12 months). Even after exclusion of this participant, mean Mlt at 12 months was still higher than the reference range (52 ± 31 days). Figure 3A–H shows the changes in static and dynamic parameters in one of the patients.

Bone tissue gene expression and protein quantification

At baseline and 12 months after ART, bone-tissue level gene expression of TNF-α, RANK, and FGF-23 genes were lower than that of our reference group (Fig. 4), without significant differences between baseline and follow-up gene expression. We did not observe significant changes in bone-tissue level protein quantification for cytokines, RANKL, OPG, FGF-23, or sclerostin after ART (Table 3). By immunohistochemistry, however, we observed an increase in OPG + osteoblasts, and a trend toward increased RANKL + osteoblasts ($p = 0.08$) and OPG + osteocytes per mm^2 of bone area ($p = 0.06$).

Correlations with BMD and histomorphometry

There were no significant correlations between changes in BMD at any site with changes in serum bone turnover markers or cytokine levels. However, 12-month percent change in femoral neck BMD was negatively correlated with the 12-month percentage change in PTH (rho −0.81, $p < 0.001$) (Fig. 1B). In a linear regression model, associations between change in femoral neck BMD and PTH remained significant after adjusting for baseline 25(OH)D and CD4 (B−0.05; 95% CI, −0.07 to−0.03; $p < 0.001$).

We explored correlations between baseline CD4, HIV RNA level, calciotropic hormones (PTH, 25(OH)D, FGF23), inflammatory markers (TNFα, IL6) and bone-specific markers (osteocalcin, P1NP, CTX, RANKL, OPG, and sclerostin), and Mlt at baseline, and found no significant correlations. Because change in OV/BV, Ob.S/BS, Oc.S/BS were the most consistent histomorphometry findings at 12 months, we explored correlations between the same list of clinical and laboratory parameters at baseline with change in OV/BV, Ob.S/BS, and Oc.S/BS. We observed negative correlations between change in OV/BV and baseline serum osteocalcin (rho −0.56, $p = 0.046$), serum P1NP (rho −0.57, $p = 0.02$), bone IL-6 (rho −0.60, $p = 0.02$), bone IL-1β (rho −0.66, $p = 0.007$), and bone RANKL (rho −0.63, $p = 0.01$). There was also a negative correlation between change in Oc.S/BS and baseline bone IL6 (−0.56, $p = 0.049$). We did not find significant correlation with change in Ob.S/BS. Last, we examined the correlation between change in PTH an change in OB/BV, Ob.S/BS, and Oc.S/BS and found no significant correlations.

Discussion

Recognizing comorbidities associated with HIV infection and its treatment is essential for adequate clinical management of PLWH. In the present study, 20% of young men with HIV had BMD below the expected range for age by DXA prior to ART initiation. BMD declined 2% to 3% at the lumbar spine and hip but not at the 1/3 distal radius after 12 months of TDF/emtricitabine (3TC)/EFV therapy. Pretreatment histomorphometry was characterized predominantly by decreased BFR/BS and increased Mlt, which was not attributable to vitamin D deficiency. After 1 year of treatment with ART, we observed no change in BV/TV and trabecular parameters, but rather, increases in Ct.Th, OV/BV, Ob.S/BS, and Oc.S/BS by histomorphometry. Contrary to our hypothesis, we did not observe changes in the main mineralization parameters (ie, Mlt, O.Th) measured by histomorphometry; furthermore, there were no significant changes in renal phosphate excretion with TDF-containing therapy. Overall, these data suggest abnormalities in bone formation and mineralization are present

in untreated PLWH without advanced HIV. With ART, there is an increase in bone remodeling, reflected by increased Ob.S/BS and Oc.S/BS, but a persistence in mineralization defect, resulting in increased OV/BV. Cortical bone appears to be relatively preserved with ART initiation, as evidenced by stable 1/3 distal radius BMD and increased Ct.Th on histomorphometry.

Serrano and colleagues[27] studied bone histomorphometry in 22 ART-naive men and women in the 1990s, one-half of whom had AIDS-defining opportunistic infections. They found that BMD by DXA and BV/TV by histomorphometry did not differ significantly from healthy controls, but bone formation parameters (OV/BV, OS/BS, O.Th, Ob.S/BS), number of osteoclasts, and dynamic parameters (BFR/BS and MS/BS) were all reduced in those with HIV infection compared to controls. Our participants had similar deficits in bone formation parameters before ART, even though they did not have advanced HIV disease (mean CD4 + of 479 cells/mm^3). Recent studies suggest that HIV proteins may have direct negative effects on human osteoblast, altering transcriptional regulation and function. In one study using human osteoblast culture, treatment with p55-gag and gp120 HIV proteins led to reduction in calcium deposition, alkaline phosphatase activity, bone morphogenetic protein (BMP)-2 and BMP-7 levels, and in the activity and expression of runt related transcription factor (RUNX)-2, which is essential for osteoblastic differentiation.[28] We also found evidence of mineralization defects in our PLWH at baseline before ART, with Mlt being higher than the reference range in 60%. Nevertheless, none of the participants in our study had increases in both Mlt and O.Th compatible with osteomalacia. Interestingly, Serrano and colleagues[27] did not find mineralization defects in their study of advanced HIV.

One year after starting TDF/3TC/EFV, we found reductions in BMD at the lumbar spine and hip, but not the 1/3 radius, without significant changes in serum levels of 1,25(OH)$_2$D, or markers of proximal tubular function, including the fractional excretion of phosphate. Contrary to our hypothesis, we did not observe significant increases in Mlt and O.Th with TDF-containing therapy. There were, however, increases in Oc.S/BS and Ob.S/BS, with an increase in OV/BV. These findings are consistent with increased bone remodeling resulting in increased unmineralized osteoid. Taken together, these findings suggest that despite increased bone remodeling with ART initiation, a persistent defect in mineralization prevented adequate mineralization of new bone resulting in decreased BMD by DXA at trabecular-predominant sites. We did not find that evidence that TDF worsened the mineralization defect, but whether or not TDF exposure contributes to the persistence of those defects is still uncertain.

In the bone remodeling cycle, the formation and subsequent mineralization of a new bone matrix orchestrated by osteoblasts occurs after the osteoclastic resorption phase. Previous studies of serum bone turnover markers in the setting of ART initiation observed that increases in bone resorption markers occurred by 3 months and preceded compensatory increases in bone formation markers that began to rise by 6 months; the resulting "catabolic window" has been suggested as a mechanism for bone loss during ART initiation.[29,30] However, at 12 months, our histomorphometry data indicated that none of the structural parameters (BV/TV, cortical and trabecular measures) were decreased in comparison to baseline, and the magnitude of increase in Ob.S/BS from baseline was greater than that of

Oc.S/BS (Table 2). We do not know whether histomorphometry from an earlier time point, at 3 or 6 months after ART initiation, would have revealed greater increase in Oc.S/BS than Ob.S/BS and decreased structural parameters, consistent with the catabolic window theory.

Of note, although we have observed increase in Ct.Th at 12 months, there was also a marginally significant increase in cortical porosity. It is recognized that mechanical properties of cortical bone are highly sensitive to variations in porosity.[31] Cortical porosity is intimately linked to the remodeling process, and serum PTH levels were associated with increased porosity of the inner cortical bone at the proximal femur and with increased odds for fractures in postmenopausal women in a recent study.[32] Deterioration in cortical microarchitecture may have a contributory role in ART-related bone loss and should be investigated in future studies.

With ART-initiation, we observed significant alterations in hormones regulating calcium and phosphate homeostasis, with a 32% increase in PTH, despite a 26% increase in 25(OH)D levels and a 13% reduction in FGF-23. Also, increases in PTH correlated with decreases in femoral neck BMD, suggesting that PTH might play a central role in the increased bone remodeling associated with ART-initiation. Elevation of PTH has been observed in other studies with initiation of TDF in people with HIV as combination ART[33,34] or in uninfected individuals as pre-exposure prophylaxis (PrEP).[35] A dose-dependent inhibition of the calcium-sensing receptor by TDF in human embryonic kidney cells was recently demonstrated and may contribute to PTH elevation in TDF-treated patients.[36] In a study evaluating the effects of vitamin D_3 supplementation in patients on various ART regimens, vitamin D_3 supplementation led to PTH decreases only in the TDF group, and this reduction occurred independent of 25(OH)D status prior to D_3 supplementation.[37] TDF use and, specifically, higher plasma concentrations of TDF have been associated with increase vitamin D binding protein (VDBP),[33,38] which might lead to functional deficiency of the active form of vitamin D by reduction in free $1,25(OH)_2D$.[38] This phenomenon may also explain, at least in part, the elevation of PTH with the use of TDF. The association between lower serum FGF-23 and higher intracellular concentration of tenofovir diphosphate was also observed in a cross-sectional analysis including patients on stable ART with a TDF-containing regimen.[38] TDF use was associated with lower FGF-23 levels in a another study including men with HIV.[39] Reduction in FGF-23, therefore, may also be related to increases in PTH observed after TDF initiation, because FGF-23 suppresses the synthesis and secretion of PTH.[40] Taken together, our results suggest that, instead of renal changes, PTH–vitamin D–FGF-23 axis dysregulation may play a central role in the early decline of BMD associated with TDF use. Although we did not observe a change in mineralization parameters in any of our participants, it is possible that some patients who experience dramatic decreases in BMD associated with TDF exposure may indeed have worsened mineralization as a result of PTH–vitamin D–FGF23 axis dysregulation and excess phosphaturia.

We observed reduced bone RANK, FGF-23, and TNF-α gene expressions in our participants with HIV to controls without HIV from our previous studies. This gene profile did not change 12 months after treatment initiation. Consistent with this finding, we did not observe changes in the quantification of bone remodeling and phosphate homeostasis-related

proteins assessed by multiplex in the bone tissue after treatment. On the other hand, negative correlations between CD4 + T cell count and serum levels of RANKL, OPG, and TNF-α (data not shown) were observed at baseline and reductions in serum RANKL and TNF-α levels were observed after ART initiation. Other studies have also found decreases in TNF-α and soluble TNF-α I and II[6,41,42] and RANKL levels,[14,41,43] with decreased[14,41] or stable OPG levels at 24 to 48 weeks after ART compared to baseline.[43] The discrepancy between serum and bone levels of OPG and RANKL also suggests that production of OPG and RANKL is not osteoblast-specific. Among other cell types, activated T cells are an important source of RANKL,[44,45] whereas B cells are recognized as OPG producers.[46] In an experimental study, increase in total splenic and bone marrow RANKL mRNA expression, concomitant with a decline in OPG mRNA expression, was observed in HIV-1 transgenic rats compared to wild-type animals.[47] The same pattern was found in purified splenic B cells from transgenic rats, suggesting a transition from OPG to RANKL production by these B cells. It is possible that changes in serum levels of RANKL and OPG we observed after ART introduction are reflective of treatment-related changes in T and B cell function, rather than in osteoblast production of these cytokines.

Our study has several limitations. For ethical reasons, it was not possible to obtain a control group of healthy individuals or patients with untreated HIV infection. In addition, we do not have a comparison group on TDF without efavirenz or on a non-TDF–containing regimen so that it is difficult to attribute findings to any specific antiretroviral. Also, we only had histomorphometry data at one time point, at 12 months after ART initiation; therefore, our data may not reflect findings during an early, potentially more dynamic, time point. Although we have used local reference values for the evaluation of static histomorphometric parameters, we do not have reference values for the dynamic parameters in the Brazilian population. Our sample size was small, but generalizable, because most patients had CD4 + T cell count> 350 cells/mm^3 and were representative of PLWH who initiate ART early in the course of HIV infection according to current guidelines.[48] In addition, only men were included, and our findings may not be representative of bone abnormalities in women with HIV infection. The strengths of our study are the inclusion of the histomorphometric study, allowing evaluation not only of structural but also of dynamic parameters, and the analysis of gene expression and quantification of proteins related with inflammation, bone remodeling, and phosphate homeostasis in the serum and the bone tissue.

In conclusion, our results suggest abnormal bone volume, turnover, and mineralization are present in PLWH before ART initiation. Treatment with TDF/3TC/EFV did not further exacerbate histomorphometric bone abnormalities. Maintenance of low BFR/BS and high Mlt, with increase in Oc.S/BS, Ob.S/BS, and OV/BV, were accompanied by decrease in lumbar spine, femoral neck, and total hip BMD and may be related to TDF-induced increases in PTH. Stable 1/3 radius BMD and increase in Ct.Th may indicate relative preservation of cortical bone with ART initiation. Future studies should focus on disentangling the effects of different antiretrovirals on histomorphometry.

Acknowledgments

References

1. Compston J HIV infection and bone disease. J Intern Med. 2016;280(4):350–358. [PubMed: 27272530]

2. Brown TT, Qaqish RB. Antiretroviral therapy and the prevalence of osteopenia and osteoporosis: a meta-analytic review. AIDS. 2006;20(17):2165–2174. [PubMed: 17086056]

3. Sharma A, Shi Q, Hoover DR, et al. Increased fracture incidence in middle-aged HIV-infected and HIV-uninfected women: updated results from the Women's Interagency HIV Study. J Acquir Immune Defic Syndr. 2015;70(1):54–61. [PubMed: 26322667]

4. Hansen AB, Gerstoft J, Kronborg G, et al. Incidence of low and high-energy fractures in persons with and without HIV infection: a Danish population-based cohort study. AIDS. 2012;26(3):285–293. [PubMed: 22095195]

5. Guerri-Fernandez R, Vestergaard P, Carbonell C, et al. HIV infection is strongly associated with hip fracture risk, independently of age, gender, and comorbidities: a population-based cohort study. J Bone Miner Res. 2013;28(6):1259–1263. [PubMed: 23362011]

6. Brown TT, McComsey GA, King MS, Qaqish RB, Bernstein BM, da Silva BA. Loss of bone mineral density after antiretroviral therapy initiation, independent of antiretroviral regimen. J Acquir Immune Defic Syndr. 2009;51(5):554–561. [PubMed: 19512937]

7. Gallant JE, Staszewski S, Pozniak AL, et al. Efficacy and safety of tenofovir DF vs stavudine in combination therapy in antiretroviral-naive patients: a 3-year randomized trial. JAMA. 2004;292(2):191–201. [PubMed: 15249568]

8. Duvivier C, Kolta S, Assoumou L, et al. Greater decrease in bone mineral density with protease inhibitor regimens compared with nonnucleoside reverse transcriptase inhibitor regimens in HIV-1 infected naive patients. AIDS. 2009;23(7):817–824. [PubMed: 19363330]

9. Rivas P, Gorgolas M, Garcia-Delgado R, Diaz-Curiel M, Goyenechea A, Fernandez-Guerrero ML. Evolution of bone mineral density in AIDS patients on treatment with zidovudine/lamivudine plus abacavir or lopinavir/ritonavir. HIV Med. 2008;9(2):89–95. [PubMed: 18093130]

10. McComsey GA, Kitch D, Daar ES, et al. Bone mineral density and fractures in antiretroviral-naive persons randomized to receive abacavir-lamivudine or tenofovir disoproxil fumarate-emtricitabine along with efavirenz or atazanavir-ritonavir: AIDS Clinical Trials Group A5224s, a substudy of ACTG A5202. J Infect Dis. 2011;203(12):1791–1801. [PubMed: 21606537]

11. Stellbrink HJ, Orkin C, Arribas JR, et al. Comparison of changes in bone density and turnover with abacavir-lamivudine versus tenofovir-emtricitabine in HIV-infected adults: 48-week results from the ASSERT study. Clin Infect Dis. 2010;51(8):963–972. [PubMed: 20828304]

12. Bhan A, Qiu S, Rao SD. Bone histomorphometry in the evaluation of osteomalacia. Bone Rep. 2018;8:125–134. [PubMed: 29955631]

13. Peach H, Compston JE, Vedi S, Horton LW. Value of plasma calcium, phosphate, and alkaline phosphatase measurements in the diagnosis of histological osteomalacia. J Clin Pathol. 1982;35(6):625–630. [PubMed: 7085914]

14. Bernardino JI, Mocroft A, Mallon PW, et al. Bone mineral density and inflammatory and bone biomarkers after darunavir-ritonavir combined with either raltegravir or tenofovir-emtricitabine in antiretroviral-naive adults with HIV-1: a substudy of the NEAT001/ANRS143 randomised trial. Lancet HIV. 2015;2(11):e464–e473. [PubMed: 26520926]

15. Karras A, Lafaurie M, Furco A, et al. Tenofovir-related nephrotoxicity in human immunodeficiency virus-infected patients: three cases of renal failure, Fanconi syndrome, and nephrogenic diabetes insipidus. Clin Infect Dis. 2003;36(8):1070–1073. [PubMed: 12684922]

16. Kinai E, Hanabusa H. Progressive renal tubular dysfunction associated with long-term use of tenofovir DF. AIDS Res Hum Retroviruses. 2009;25(4):387–394. [PubMed: 19361280]

17. Maggi P, Montinaro V, Bellacosa C, et al. Early markers of tubular dysfunction in antiretroviral-experienced HIV-infected patients treated with tenofovir versus abacavir. AIDS Patient Care STDS. 2012;26(1):5–11 [PubMed: 22136504]

18. Dauchy FA, Lawson-Ayayi S, de LaFaille R, et al. Increased risk of abnormal proximal renal tubular function with HIV infection and antiretroviral therapy. Kidney Int. 2011;80(3):302–309. [PubMed: 21544066]

19. Yin MT, Overton ET. Increasing clarity on bone loss associated with antiretroviral initiation. J Infect Dis. 2011;203(12):1705–1707. [PubMed: 21606527]

20. McComsey GA, Tebas P, Shane E, et al. Bone disease in HIV infection: a practical review and recommendations for HIV care providers. Clin Infect Dis. 2010;51(8):937–946. [PubMed: 20839968]

21. Shepherd JA, Lu Y, Wilson K, et al. Cross-calibration and minimum precision standards for dual-energy X-ray absorptiometry: the 2005 ISCD Official Positions. J Clin Densitom. 2006;9(1):31–36. [PubMed: 16731429]

22. Shepherd JA, Schousboe JT, Broy SB, Engelke K, Leslie WD. Executive Summary of the 2015 ISCD Position Development Conference on Advanced Measures From DXA and QCT: Fracture Prediction Beyond BMD. J Clin Densitom. 2015;18(3):274–286. [PubMed: 26277847]

23. Dempster DW, Compston JE, Drezner MK, et al. Standardized nomenclature, symbols, and units for bone histomorphometry: a 2012 update of the report of the ASBMR Histomorphometry Nomenclature Committee. J Bone Miner Res. 2013;28(1):2–17. [PubMed: 23197339]

24. Dos Reis LM, Batalha JR, Munoz DR, et al. Brazilian normal static bone histomorphometry: effects of age, sex, and race. J Bone Miner Metab. 2007;25(6):400–406. [PubMed: 17968492]

25. Melsen F, Mosekilde L. Tetracycline double-labeling of iliac trabecular bone in 41 normal adults. Calcif Tissue Res. 1978;26(2):99–102. [PubMed: 737565]

26. Gomes SA, dos Reis LM, deOliveira IB, Noronha IL, Jorgetti V, Heilberg IP. Usefulness of a quick decalcification of bone sections embedded in methyl methacrylate[corrected]: an improved method for immunohistochemistry. J Bone Miner Metab. 2008;26(1):110–113. [PubMed: 18095073]

27. Serrano S, Marinoso ML, Soriano JC, et al. Bone remodelling in human immunodeficiency virus-1-infected patients. A histomorphometric study. Bone. 1995;16(2):185–191. [PubMed: 7756046]

28. Cotter EJ, Malizia AP, Chew N, Powderly WG, Doran PP. HIV proteins regulate bone marker secretion and transcription factor activity in cultured human osteoblasts with consequent potential implications for osteoblast function and development. AIDS Res Hum Retroviruses. 2007;23(12):1521–1530. [PubMed: 18160010]

29. Boyce BF, Xing L. Biology of RANK, RANKL, and osteoprotegerin. Arthritis Res Ther. 2007;9(Suppl 1):S1. [PubMed: 17634140]

30. Cotter AG, Mallon PW. The effects of untreated and treated HIV infection on bone disease. Curr Opin HIV AIDS. 2014;9(1):17–26. [PubMed: 24263798]

31. Schaffler MB, Burr DB. Stiffness of compact bone: effects of porosity and density. J Biomech. 1988;21(1):13–16. [PubMed: 3339022]

32. Osima M, Borgen TT, Lukic M, et al. Serum parathyroid hormone is associated with increased cortical porosity of the inner transitional zone at the proximal femur in postmenopausal women: the Tromso Study. Osteoporos Int. 2018;29(2):421–431. [PubMed: 29134242]

33. Hsieh E, Fraenkel L, Han Y, et al. Longitudinal increase in vitamin D binding protein levels after initiation of tenofovir/lamivudine/efavirenz among individuals with. HIV. AIDS. 2016;30(12):1935–1942. [PubMed: 27124896]

34. Masia M, Padilla S, Robledano C, Lopez N, Ramos JM, Gutierrez F. Early changes in parathyroid hormone concentrations in HIV-infected patients initiating antiretroviral therapy with tenofovir. AIDS Res Hum Retroviruses. 2012;28(3):242–246. [PubMed: 21639815]

35. Havens PL, Stephensen CB, VanLoan MD, et al. Decline in bone mass with tenofovir disoproxil fumarate/emtricitabine is associated with hormonal changes in the absence of renal impairment when used by HIV-uninfected adolescent boys and young men for HIV preexposure prophylaxis. Clin Infect Dis. 2017;64(3):317–325. [PubMed: 28013265]

36. Mingione A, Maruca K, Chiappori F, et al. High parathyroid hormone concentration in tenofovir-treated patients are due to inhibition of calcium-sensing receptor activity. Biomed Pharmacother. 2018;97:969–974. [PubMed: 29136775]

37. Havens PL, Stephensen CB, Hazra R, et al. Vitamin D3 decreases parathyroid hormone in HIV-infected youth being treated with tenofovir: a randomized, placebo-controlled trial. Clin Infect Dis. 2012;54(7):1013–1025. [PubMed: 22267714]

38. Havens PL, Kiser JJ, Stephensen CB, et al. Association of higher plasma vitamin D binding protein and lower free calcitriol levels with tenofovir disoproxil fumarate use and plasma and intracellular tenofovir pharmacokinetics: cause of a functional vitamin D deficiency? Antimicrob Agents Chemother. 2013;57(11):5619–5628. [PubMed: 24002093]

39. Wang R, Shlipak MG, Ix JH, et al. Association of fibroblast growth factor-23 (FGF-23) with incident frailty in HIV-infected and HIV-uninfected individuals. J Acquir Immune DeficSyndr.2019;80(1):118–125.

40. Blau JE, Collins MT. The PTH-Vitamin D-FGF23 axis. Rev Endocr Metab Disord. 2015;16(2):165–174. [PubMed: 26296372]

41. Brown TT, Ross AC, Storer N, Labbato D, McComsey GA. Bone turnover, osteoprotegerin/RANKL and inflammation with antiretroviral initiation: tenofovir versus non-tenofovir regimens. Antivir Ther. 2011;16(7):1063–1072. [PubMed: 22024522]

42. Aukrust P, Muller F, Lien E, et al. Tumor necrosis factor (TNF) system levels in human immunodeficiency virus-infected patients during highly active antiretroviral therapy: persistent TNF activation is associated with virologic and immunologic treatment failure. J Infect Dis. 1999;179(1):74–82. [PubMed: 9841825]

43. Kelesidis T, Moser CB, Johnston E, et al. Brief Report: Changes in plasma RANKL-osteoprotegerin in a prospective, randomized clinical trial of initial antiviral therapy: A5260s. J Acquir Immune Defic Syndr. 2018;78(3):362–366. [PubMed: 29533303]

44. Weitzmann MN, Cenci S, Rifas L, Haug J, Dipersio J, Pacifici R. T cell activation induces human osteoclast formation via receptor activator of nuclear factor kappaB ligand-dependent and -independent mechanisms. J Bone Miner Res. 2001;16(2):328–337. [PubMed: 11204433]

45. Weitzmann MN, Cenci S, Rifas L, Brown C, Pacifici R. Interleukin-7 stimulates osteoclast formation by up-regulating the T-cell production of soluble osteoclastogenic cytokines. Blood. 2000;96(5):1873–1878. [PubMed: 10961889]

46. Yun TJ, Chaudhary PM, Shu GL, et al. OPG/FDCR-1, a TNF receptor family member, is expressed in lymphoid cells and is up-regulated by ligating CD40. J Immunol. 1998;161(11):6113–6121. [PubMed: 9834095]

47. Vikulina T, Fan X, Yamaguchi M, et al. Alterations in the immuno-skeletal interface drive bone destruction in HIV-1 transgenic rats. Proc Natl Acad Sci U S A. 2010;107(31):13848–13853. [PubMed: 20643942]

48. World Health Organization Consolidated guidelines on the use of antiretroviral drugs for treating and preventing HIV infection: recommendations for a public health approach. Geneva. World Health Organization 2016 [cited 2019 May 10]. Available from: http://en.eecaac2018.org/world/who-guidelines-on-the-use-of-arv-drugs-for-treating-and-preventing-hiv-infection-second-edition/
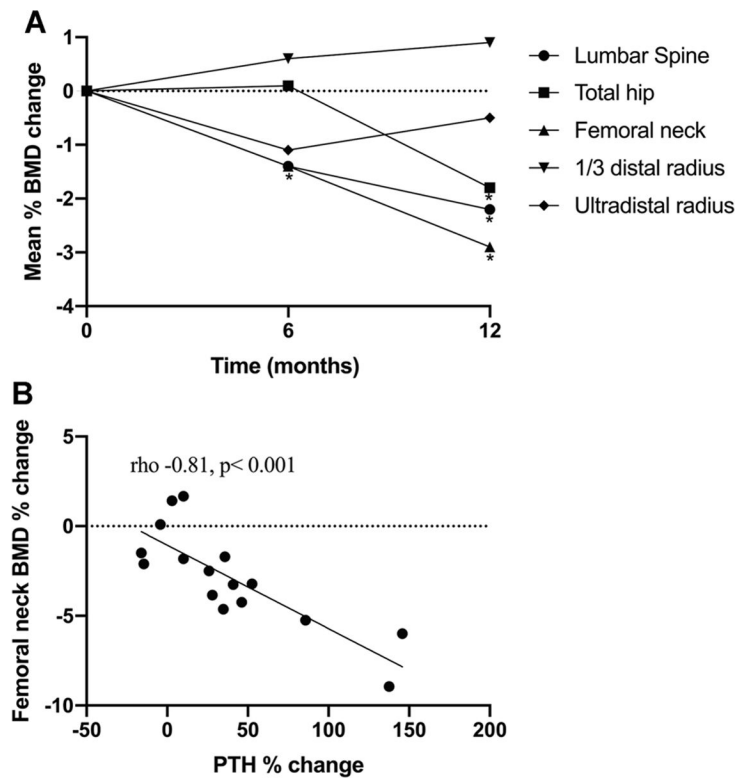
Fig. 1.
BMD change and its association with PTH change. (*A*) Percentage change in BMD by DXA with ART initiation ($n = 16$). There was a significant decline in femoral neck at 6 months. After 1 year, BMD decreased approximately 2.1% at the lumbar spine, 2.8% at the femoral neck, and 1.8% at the total hip. No significant changes were seen in 1/3 distal radius BMD. (*B*) Correlation between percentage change in femoral neck BMD and 1-year percentage change in PTH. The greater the PTH increase, the greater the bone loss at femoral neck.
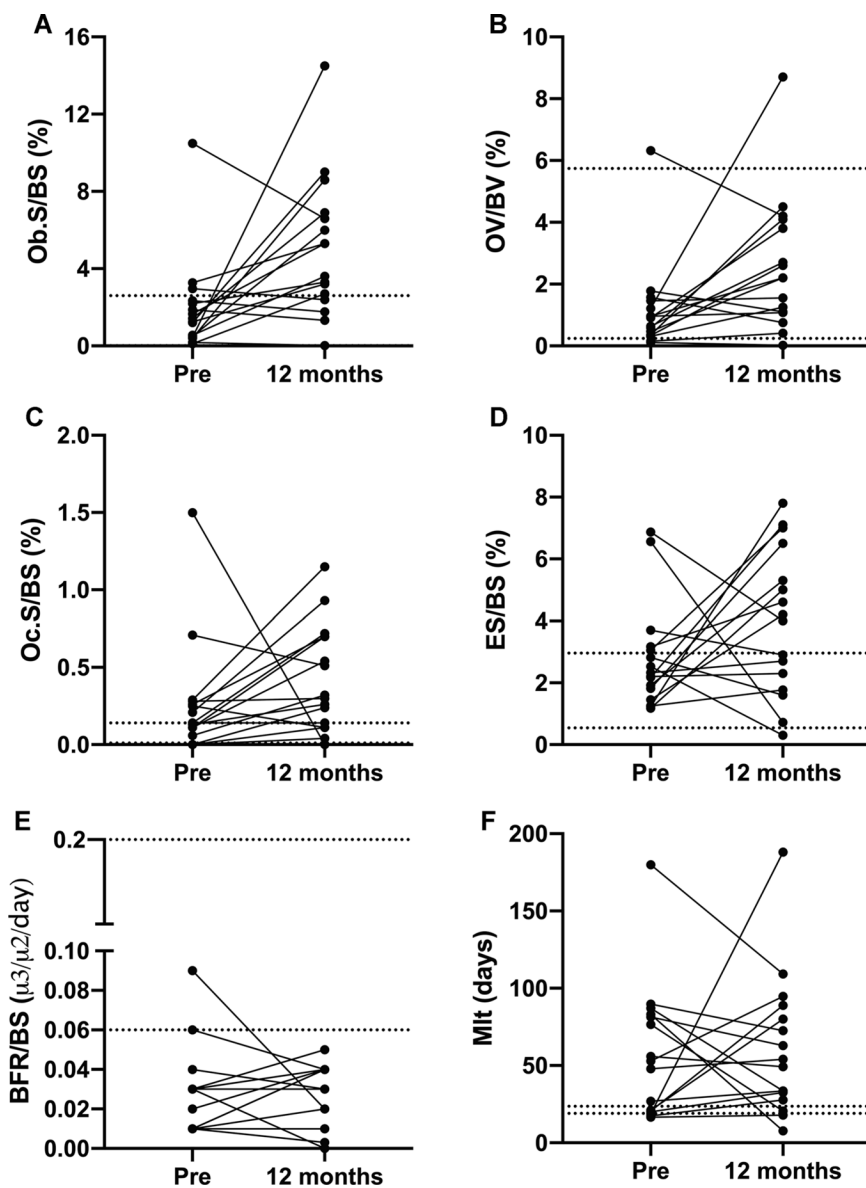
Fig. 2.
Individual changes in histomorphometric parameters. Despite significant increases in OV/BV, Ob.S/BS, and Oc.S/BS, we observed impressive interindividual variation in histomorphometric parameters. ES/BS = eroded surface; BFR/BS = bone formation rate; Mlt = mineralization lag time; OV/ BV = osteoid volume; Ob.S/BS = osteoblast surface; Oc.S/BS = osteoclast surface.
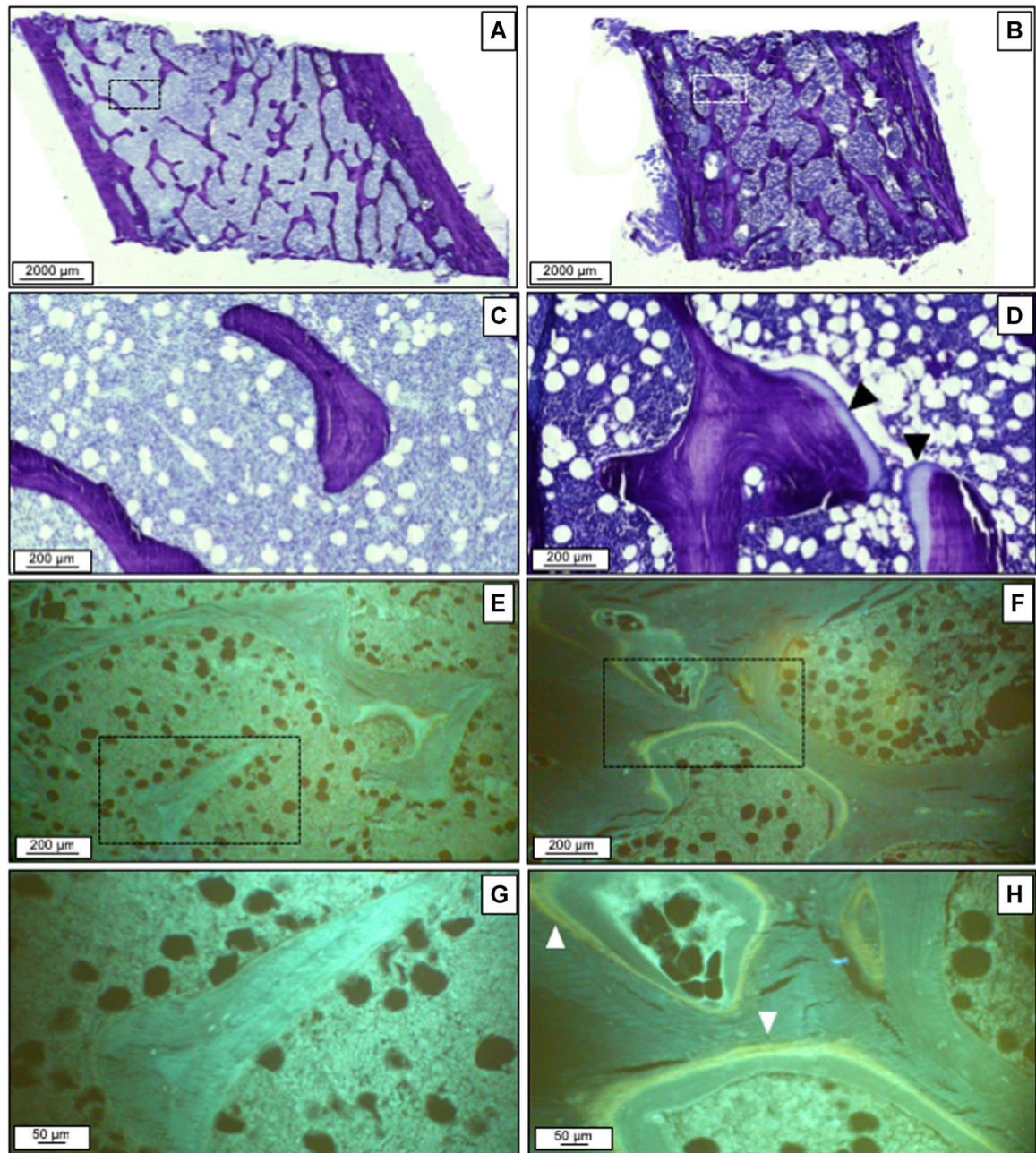
Fig. 3.
Static and dynamic parameters change after therapy. Histomorphometric parameters before (*A, C, E, G*) and after therapy (*B, D, F, H*) in an individual patient. Toluidine blue staining shows decreased connectivity and low cellular parameters at baseline (*A, C*). After 1 year, there was an increase in osteoid (black arrowheads). There were no tetracycline labels at baseline (*E, G*). At 1 year, some single-labels and double-labels (white arrowheads) were seen.
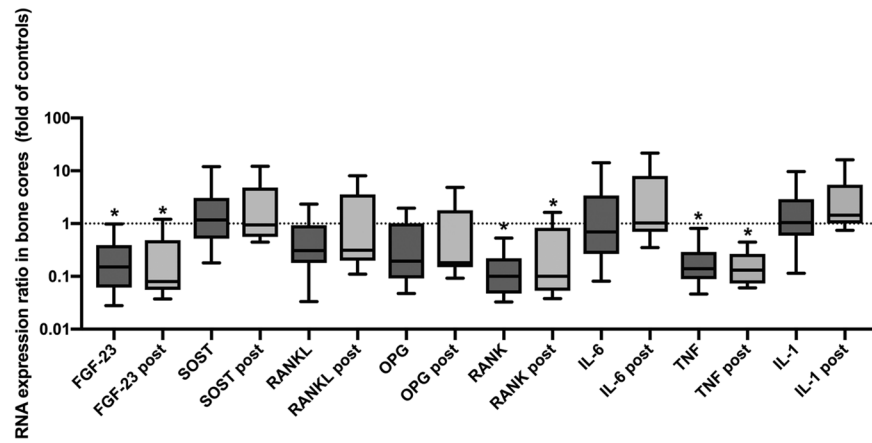
Fig. 4.
Relative bone-tissue gene expression at baseline and 12 months post-ART. Box plot of bone-tissue gene expression relative to controls for baseline and 12-month time points. The upper and lower whiskers represent the 10th and 90th percentiles. Statistical differences in gene expression relative to controls are represented by asterisks.

Table 1.

HIV and Immune Parameters, Calciotropic Hormones, Bone Turnover Markers, and Renal Markers Before and 12 Months After ART ($n = 16$)

	Pre-ART	Post-ART	*p*
HIV and immune parameters			
CD4 + T cell (cells/mm³)	479 ± 189	739 ± 232	**< 0.001**
TNF-α (pg/mL)	2.29 (1.78–3.37)	1.61 (1.42 – 2.05)	**0.03**
IL-6 (pg/mL)	1.32 (0.76–2.56)	1.02 (0.93 – 1.11)	0.06
Calciotropic hormones			
25(OH)D (ng/mL)	22.0 ± 7.0	27.7 ± 8.7	**0.04**
1,25(OH)$_2$D (pg/mL)	51.7 ± 10.3	58.2 ± 20.2	0.20
Intact PTH (pg/mL)	31.3 ± 9.2	41.4 ± 12.4	**0.004**
FGF-23 (pg/mL)	28.29 (26.20 – 34.88)	24.67 (22.18 – 28.29)	**0.04**
Renal markers			
Serum creatinine (mg/dL)	0.91 (0.87 – 1.02)	0.89 (0.81 – 0.97)	0.54
Serum HCO$_3^-$	26.5 ± 2.3	25.4 ± 2.0	0.15
Serum uric acid (mg/dL)	5.4 ± 0.8	4.8 ± 0.9	**0.02**
Serum PO$_4^-$ (mg/dL)	3.6 (3.1 – 4.0)	3.5 (3.2 – 4.1)	0.38
uProt/Cr (g/g)	0.07 (0.05 – 0.10)	0.07 (0.06 – 0.08)	0.78
uβ2MG/Cr (µg/g)	57.2 (45.5 – 124.9)	63.4 (35.3 – 163.4)	0.33
FEP (%)	13.0 ± 4.4	12.2 ± 3.2	0.509
FEAU (%)	5.3 (4.3 – 7.1)	6.1 (4.8 – 8.9)	0.26
Bone turnover markers, sclerostin, and RANKL/OPG cytokines			
Osteocalcin (ng/mL)	18.0 ± 5.2	24.8 ± 5.5	**0.002**
CTX (ng/mL)	0.44 ± 0.23	0.51 ± 0.24	0.45
P1NP (ng/mL)	63.7 ± 28.8	79.7 ± 30.8	0.09
Sclerostin (pg/mL)	1206 (603.4 – 2463)	2027 (1705 – 2308)	0.19
RANKL (pg/mL)	15.24 (9.98 – 21.87)	10.86 (7.46 – 16.82)	**0.049**
OPG (pg/mL)	168.92(145.1 – 266.6)	214.5 (138.9 – 260.9)	0.39
Bone mineral density			
Lumbar spine BMD (g/cm²)	0.981 ± 0.094	0.960 ± 0.110	0.048
Femoral neck BMD (g/cm²)	0.887 ± 0.145	0.862 ± 0.145	0.001

	Pre-ART	Post-ART	*p*
Total hip BMD (g/cm^2)	1.029 ± 0.138	1.010 ± 0.138	0.04

Values are mean ± SD or median (IQR). Bold *p* values are < 0.05.

25(OH)D = 25-hydroxy-vitamin D; 1,25(OH)2D = 1,25-dihidroxi-vitamin D; PTH = parathyroid hormone; uProt/Cr = urinary protein to creatinine ratio; uβ2MG/Cr = urinary protein to creatinine ratio; FEP = fractional excretion of phosphate; FEAU = fractional excretion of uric acid; CTX = C-terminal telopeptide of type 1 collagen; P1NP = N-terminal propeptide of type 1 collagen; BMD = bone mineral density.

Table 2.

Histomorphometry Before and 12 Months After ART ($n = 16$)

	Pre-ART	Post-ART	p	Reference values [a]
Structural parameters				
Bone volume/total volume (%)	23.5 ± 6.5	21.0 ± 6.1	0.25	24.0 ± 6.1
Cortical thickness (µm)	646.5 ± 177.0	886.9 ± 349.4	**0.04**	> 520
Cortical porosity (%)	4.07 ± 1.51	6.34 ± 3.54	0.05	< 10
Trabecular thickness (µm)	141.2 ± 25.8	134.8 ± 33.6	0.33	127.9 ± 29.7
Trabecular separation (µm)	486 (357 – 562)	498 (418 – 586)	0.57	420.6 ± 124.1
Trabecular number (#/mm)	1.66 ± 0.36	1.55 ± 0.27	0.34	1.89 ± 0.42
Bone formation parameters				
Osteoid thickness (µm)	8.05 (7.20 – 8.99)	9.4 (6.5 – 11.08)	1.00	11.7 ± 3.5
Osteoid volume/bone volume (%)	0.77 (0.35 – 1.40)	2.2 (1.09 – 4.03)	**0.02**	2.99 ± 2.75
Osteoid surface/bone surface (%)	12.2 ± 7.4	15.6 ± 10.2	0.28	16.1 ± 12.6
Osteoblastic surface/bone surface (%)	1.33 (0.46 – 2.30) [b]	4.45 (2.48 – 6.83) [b]	**0.02**	1.2 ± 1.4
Bone resorption parameters				
Osteoclastic surface/bone surface (%)	0.14 (0.07 – 0.27)	0.31 (0.12 – 0.7) [b]	**0.04**	0.03 ± 0.11
Eroded surface/bone surface (%)	2.26 (1.54 – 3.14)	4.1 (1.90 – 6.2) [b]	0.15	1.75 ± 1.21
Dynamic parameters				
Mineralizing surface/bone surface (%)	3.6 ± 2.5 [b]	3.7 ± 1.9 [b]	0.90	18.3 ± 7.5
Mineral apposition rate (µm/day)	0.65 (0.54 – 0.86)	0.73 (0.62 – 0.89)	0.84	0.65 (0.54 – 0.86)
Bone formation rate (µm³/µm²/day)	0.02 (0.01 – 0.03) [b]	0.03 (0.01 – 0.04) [b]	0.30	0.13 ± 0.07
Mineralization lag time (days)	50.4 (20.2 – 82.6) [b]	51.7 (28.9 – 86.7) [b]	1.00	21.3 ± 2.3

Values are mean ± SD or median (IQR). Bold p values are < 0.05.

[a] Reference populations obtained from Melsen and Mosekilde[25] and Gomes and colleagues.[26]

[b] Median or mean value below or 1 SD above reference values.

Table 3.

Bone-Tissue Level Protein Quantification for Cytokines, FGF-23, and Sclerostin Levels by Multiplex and Bone Cell Expression of RANKL and OPG by Immunohistochemistry Before and 12 Months After ART ($n = 16$)

	Pre-ART	12 months post-ART	p
Bone protein quantification by multiplex			
TNF-α (pg/mg)	0.14 ± 0.05	0.16 ± 0.12	0.56
IL-6 (pg/mg)	0.45 ± 0.17	0.48 ± 0.27	0.82
IL-1β (pg/mg)	0.38 ± 0.15	0.46 ± 0.30	0.45
RANKL (pg/mg)	1.82 ± 0.82	1.99 ± 1.51	0.74
OPG (pg/mg)	14.72 ± 8.14	16.99 ± 12.33	0.58
FGF-23 (pg/mg)	17.57 (13.17–24.02)	14.63 (9.75–22.08)	0.87
Sclerostin (pg/mg)	2813 ± 1805	2639 ± 1328	0.73
Bone cell expression of RANKL and OPG by immunohistochemistry			
RANKL + osteocytes	0.90 (0.49–1.74)	1.43 (0.43–7.08)	0.28
OPG + osteocytes	0.33 (0.14–0.88)	0.83 (0.29–3.98)	0.06
OPG + /RANKL + ratio osteocytes	0.25 (0.09–1)	1 (0.45–2)	0.15
RANKL + osteoblasts and lining cells	2.94 (0.58–5.99)	6.01 (3.86–10.70)	0.08
OPG + osteoblasts and lining cells	2.31 (1.05–3.16)	5.57 (3.66–13.12)	**0.02**
OPG + /RANKL + ratio osteoblasts and lining cells	0.79 (0.49–1.82)	1.13 (0.74–1.90)	0.80

Values are mean ± SD or median (IQR). Bold p values are < 0.05.

FGF-23 = fibroblast growth factor-23; RANKL = receptor activator of nuclear factor kappa-B ligand; OPG = osteoprotegerin; TNF-α = tumor necrosis factor-α; IL-6 = interleukin-6; IL-1β = interleukin-1β.